Chemical Science

ROYAL SOCIETY OF CHEMISTRY

EDGE ARTICLE

View Article Online
View Journal | View Issue

Cite this: *Chem. Sci.*, 2022, **13**, 5893

All publication charges for this article have been paid for by the Royal Society of Chemistry

Received 16th February 2022
Accepted 6th April 2022

DOI: 10.1039/d2sc00990k

rsc.li/chemical-science

Crystallization induced room-temperature phosphorescence and chiral photoluminescence properties of phosphoramides†

Satyam Jena,[a] Jusaina Eyyathiyil,[a] Santosh Kumar Behera,[a] Maho Kitahara,[b] Yoshitane Imai *[b] and Pakkirisamy Thilagar *[a]

We report the design and synthesis of a series of room temperature phosphorescent phosphoramides **TPTZPO**, **TPTZPS**, and **TPTZPSe** with a donor (phenothiazine)–acceptor (P = X, X = O, S, and Se) architecture. All the compounds show structureless fluorescence with a nanosecond lifetime in dilute solutions. However, these compounds show dual fluorescence and room temperature phosphorescence (RTP) in the solid state. Both the intensity and energy of luminescence depend on the heteroatom attached to the phosphorus center. For example, compound **TPTZPO** with the P=O unit exhibits fluorescence at a higher energy region than **TPTZPS** and **TPTZPSe** with the P=S and P=Se groups, respectively. Crystalline samples of **TPTZPO**, **TPTZPS**, and **TPTZPSe** show stronger RTP than the amorphous powder of respective compounds. Detailed steady-state, time-resolved photoluminescence and computational studies established that the ^{3}n–π* state dominated by the phenothiazine moiety is the emissive state of these compounds. Although **TPTZPS** and **TPTZPSe** crystallized in the chiral space group, only **TPTZPSe** showed chiroptical properties in the solid state. The luminescence dissymmetry factor (g_{lum}) value of **TPTZPS** is small and below the detection limit, and a CPL spectrum could not be observed for this compound.

1. Introduction

Room temperature phosphorescent (RTP) materials have attracted considerable research attention owing to their potential applications in organic light-emitting diodes (OLEDs),[1–9] sensing,[10–13] and time-gated bio-imaging applications.[14–21] Phosphorescence is the spin forbidden radiative decay of triplet excitons to the ground singlet state ($T_1 \rightarrow S_0$). The efficiency of RTP is dependent on the $S_n \rightarrow T_n$ intersystem crossing (ISC); the efficiency of ISC depends on the spin–orbit coupling (SOC). Thus, in the past, the development of RTP materials was mainly limited to only transition metal complexes (*e.g.* iridium(III), platinum(II), gold(III), ruthenium(II), and copper(I)).[22–33]

Recently, enormous research efforts have been devoted to developing metal-free organic phosphors because of their low toxicity and environmentally benign nature compared to their inorganic counterparts. However, organic phosphors exhibit weak luminescence with low phosphorescence quantum yield under ambient conditions due to weak SOC, inefficient intersystem crossing, and poor radiative $T_1 \rightarrow S_0$ transition.[34,35] Thus, developing organic phosphors with improved phosphorescence quantum yield is an important and challenging area of research. Innovative techniques such as crystallization-induced phosphorescence, doping in a rigid host (polymer matrices), aggregates, and multi-component molecular hybrids have been successfully explored for developing efficient RTP materials by reducing the non-radiative deactivation of triplet excitons.[36–47]

On the other hand, incorporating main-group elements such as B, Si, N, P, O, S, and halogens in organic backbones provides a new strategy to achieve functional molecules.[35,48–76] Recently, finetuning the interactions between orbitals of different symmetry in heteroatom doped organic luminophores has attracted considerable attention for developing RTP materials. Not long ago, Huang and co-workers developed strongly emissive RTP materials by finetuning the interactions between sulfur and oxygen in oxidized phenothiazine derivatives.[77] Despite these developments, bright phosphorescence at room temperature is rarely observed in molecules with lighter elements.

We have been involved in developing multi-functional molecules by constraining their molecular conformations.[78–81] During these studies, we observed that the conformation of the molecule plays a significant role in controlling the energy and

[a]*Department of Inorganic and Physical Chemistry, Indian Institute of Science Bangalore, India – 560012. E-mail: thilagar@iisc.ac.in*

[b]*Department of Applied Chemistry, Faculty of Science and Engineering, Kindai University, 3-4-1 Kowakae, Higashi-Osaka, Osaka 577-8502, Japan. E-mail: y-imai@apch.kindai.ac.jp*

† Electronic supplementary information (ESI) available. CCDC 1977279, 1916761 and 1916789. For ESI and crystallographic data in CIF or other electronic format see https://doi.org/10.1039/d2sc00990k

mixing of the electronically excited states, thereby curbing the undesirable non-radiative decay channels that are detrimental to the PL quantum yield.[82,83] As part of the ongoing program, we designed and synthesized phosphoramides (**TPTZPO**, **TPTZPS** and **TPTZPSe**), keeping in view that the nonplanar heterocycle phenothiazine would enhance spin–orbit coupling through the mixing of molecular orbitals with different symmetry.[84–94] Further, covalently linking a P = X (X = O/S/Se) group to phenothiazine can enhance the spin–orbit coupling (SOC) and intersystem crossing *via* n–π* interactions. We also envisioned that the nonplanar structure of phenothiazine and the tetrahedral geometry imposed by the phosphorus center may curb the unwarranted intermolecular interactions and lead to molecules with improved RTP characteristics. As anticipated, RTP was realized with these compounds. Compounds **TPTZPS** and **TPTZPSe** crystallized in the enantiomerically pure chiral space group $P2_1$, and their chiroptical properties were measured. All these results are reported in this article.

2. Results and discussion

Compounds **TPTZPO**, **TPTZPS**, and **TPTZPSe** were synthesized following the literature procedures.[63,95,96] The addition of *n*-BuLi to anhydrous THF solution of phenothiazine under stirring conditions generated a N-centered anion, and the subsequent trapping of the anion with phosphorus trichloride gave tris-phenothiazinephosphine as a colorless solid. Oxidation of tris-phenothiazinephosphine with H_2O_2/S-powder/Se-powder yielded **TPTZPO**, **TPTZPS**, and **TPTZPSe**, respectively (Scheme 1). Analytically pure **TPTZPO**, **TPTZPS** and **TPTZPSe** were obtained by repeated recrystallization in a hexane and ethyl acetate solvent mixture (95 : 5). All the compounds were stable under ambient conditions. Compound **TPTZPO** melts at 192–195 °C; in contrast, **TPTZPS** and **TPTZPSe** decompose at 190 °C.

All compounds were characterized by NMR (^{1}H, ^{31}P), HRMS, elemental analysis, and high-performance liquid chromatography (HPLC) (Fig. 1 and S1–S8†). The molecular structures of all the compounds were confirmed by single-crystal X-ray diffraction studies.

Compounds **TPTZPO**, **TPTZPS**, and **TPTZPSe** show broad ^{1}H NMR resonance at 25 °C in $CDCl_3$, CD_2Cl_2, DMSO-d_6, and THF-d_8. Upon decreasing the temperature, the ^{1}H resonances are resolved for compounds **TPTZPS** and **TPTZPSe**, while those of **TPTZPO** are not resolved even at −90 °C in CD_2Cl_2. The two peaks observed for **TPTZPO** at 25 °C merged to a single broad peak at −10 °C, and as temperature decreased further, it started to split (Fig. S1†). In total twelve ^{1}H resonances appeared at −90 °C for **TPTZPO**, indicating the asymmetry in the system.

However, broad NMR signals started to split at 0 °C, and a total of thirteen well-resolved peaks appeared at −90 °C for **TPTZPS** and **TPTZPSe**, respectively (Fig. 1 and S2†). These results indicated that the phenothiazine rings in **TPTZPO**, **TPTZPS**, and **TPTZPSe** undergo dynamic flip-flap motion at the NMR timescale. The ^{1}H resonances are broad peaks even at −90 °C for **TPTZPO**, indicating the greater extent of phenothiazine ring dynamics. The shorter P═O bond distance may be the root cause for the observed larger ring flipping in **TPTZPO**. The free energy of activation for the hindered rotation was calculated using the Gutowsky–Holm equation. $\Delta G^{\#} = 0.00457T_c(9.97 + \log(T_c/\Delta\delta))$.[97] Where $\Delta\delta$ is the maximum difference between the two peaks at low temperature and T_c is the coalescence temperature (273 K) (calculation details are given in the ESI†). The free energy calculated for the rotational barrier in **TPTZPS** and **TPTZPSe** was 16.78 kcal mol^{-1} and 16.50 kcal mol^{-1}, respectively.

The ^{31}P NMR chemical shifts for **TPTZPO** (0.6 ppm), **TPTZPS** (54.5 ppm), and **TPTZPSe** (49.4 ppm) are in the region expected for compounds with P = X (O, S, and Se) moieties reported in the literature.[98,99] Compounds **TPTZPO**, **TPTZPS**, and **TPTZPSe** show the $(M + Na)^+$ peak at 664.0718, 680.0489, and 727.9936, respectively, under HRMS conditions, and these values are consistent with their molecular compositions.

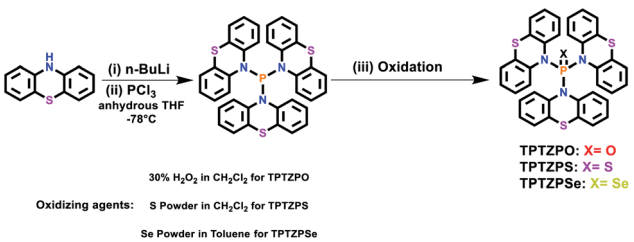

Scheme 1 Synthesis of TPTZPO, TPTZPS and TPTZPSe. (i) *n*-BuLi, −78 °C, anhydrous THF, 1 h; (ii) PCl_3, temperature: 298 K; (iii) 30% H_2O_2 in dichloromethane for TPTZPO, sulfur powder in dichloromethane for TPTZPS and selenium powder in toluene for TPTZPSe.

2.1 Crystal structure

The molecular structures of **TPTZPO**, **TPTZPS**, and **TPTZPSe** were confirmed by single-crystal X-ray diffraction (SCXRD) studies. Compound **TPTZPO** crystallized in the monoclinic crystal system with the centrosymmetric $C2/c$ space group, while **TPTZPS** and **TPTZPSe** crystallized in the monoclinic chiral $P2_1$ space group (Table S1†). In all the compounds, the phosphorus centers adopted distorted tetrahedral geometries, and the P = X (X = O, S or Se) fragment is surrounded by three phenothiazine units (Fig. 1). The N–P bond lengths are in the range of 1.668–1.689 Å which are longer than the typical N═P bond (1.58 Å) and shorter than the P–N single bond (1.76 Å) (Table S2†), a feature typical of P–N resonance double bond distances observed in phosphoramides.[62,63,99,100]

Interestingly, compounds **TPTZPO**, **TPTZPS**, and **TPTZPSe** with nonplanar phenothiazine (PTZ) donors show shorter P–N bonds than phosphoramides with planar carbazole (CBZ) donors reported elsewhere.[62,63] This can be attributed to the strong electron-donating capacity of PTZ compared to CBZ. In all the compounds, the phenothiazine units were nonplanar, and each phenothiazine moiety was puckered uniquely against the P = X axis and showed a distinct puckering angle. The P–N bond distances were influenced by the degree of puckering of the phenothiazine moiety in these compounds; the more significant the puckering angle the shorter the P–N bond (Table S2†). Compounds **TPTZPO**, **TPTZPS**, and **TPTZPSe** generate

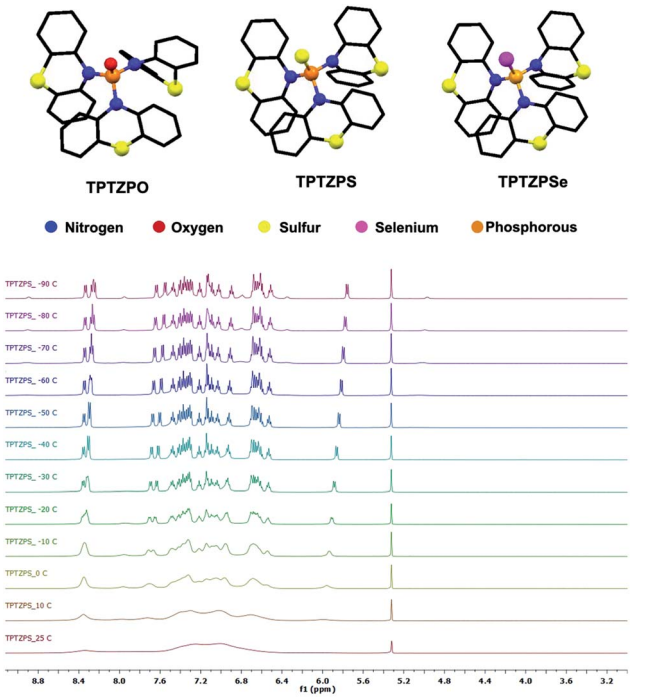

Fig. 1 Molecular structures of TPTZPO, TPTZPS and TPTZPSe with atom colour code (hydrogen atoms are removed for clarity) (top). Variable temperature ^{1}H NMR spectra of compound TPTZPS in the range of 25 °C to −90 °C (10 °C interval) recorded in CD_2Cl_2 (bottom).

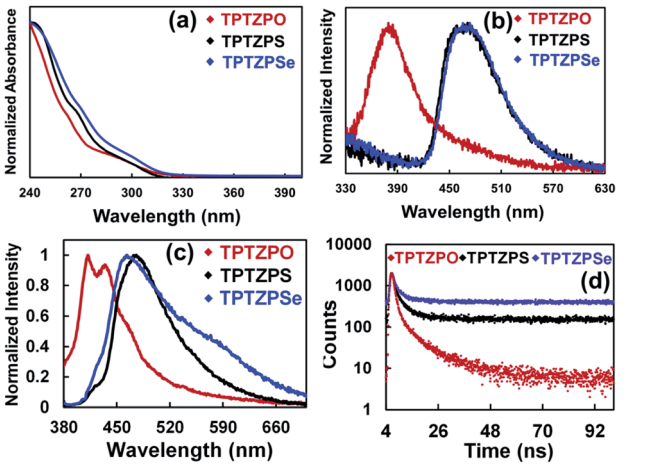

Fig. 2 (a) Normalized UV-visible absorption spectra (conc. 10^{-5} M). (b) Normalized photoluminescence spectra of TPTZPO, TPTZPS, and TPTZPSe in dichloromethane (conc. 10^{-4} M), λ_{ex} = 280 nm. (c) Normalized photoluminescence spectra of pristine solids of these compounds (λ_{ex} = 360 nm). (d) Solid-state photoluminescence decay plot (λ_{ex} = 375 nm and λ_{em} = 550 nm) of these compounds. The incomplete decay of TPTZPS and TPTZPSe indicates the existence of a long-lived species.

supramolecular structures facilitated *via* intermolecular P = X···H–C and S···H–C interactions between neighboring molecules in the solid-state. In the case of **TPTZPS** and **TPTZPSe**, the supramolecular structures are further augmented by intermolecular C–H···π interactions between the phenothiazine moieties of the neighboring molecules (Fig. S9–S11†). Such interactions are absent in **TPTZPO**. As anticipated, intermolecular face-to-face π···π interactions were not found in **TPTZPO**, **TPTZPS**, and **TPTZPSe**. Thus, these compounds are expected to show strong luminescence in the solid state.

2.2 Optical properties

Dichloromethane (DCM) solutions (conc. 10^{-5} M) of **TPTZPO**, **TPTZPS**, and **TPTZPSe** exhibit a broad absorption band in the region 250–330 nm (Fig. 2a). No shift in the absorption maxima concerning P=O, P=S, and P=Se units indicated that the electronic communication between the phenothiazine and P = X unit is negligible in the ground state. This observation parallels the UV-Vis spectra of tris-carbazole phosphoramides reported by Huang *et al.*[95,98] The absorption process in **TPTZPO**, **TPTZPS**, and **TPTZPSe** is insensitive to the solvent polarity indicating the nonpolar electronic ground state in these compounds.

DCM solutions of these compounds showed a structureless broad peak in the region 330–500 nm (Fig. 2b). Compounds **TPTZPS** (λ_{em} = ∼470 nm) and **TPTZPSe** (λ_{em} = ∼470 nm) showed red-shifted emission compared to **TPTZPO** (λ_{em} = ∼380 nm). The PL peak position in these compounds is independent of the excitation wavelength; in contrast, the PL intensity depends on the excitation wavelength, and the maximum intensity was observed for λ_{ex} = 280 nm (Fig. S12†). The excitation spectra of these compounds reproduced the corresponding absorption spectra (Fig. S13†). Furthermore, the PL peak maxima of these compounds are unchanged as the concentration of the solutions increased from 10^{-6} molar to 10^{-4} molar (Fig. S14†), and the maximum intensity was observed for 10^{-4} molar solutions. Like absorption spectra, the emission spectrum of **TPTZPO** was insensitive to the solvent polarity (Fig. S15†). However, the λ_{em} values of **TPTZPS** and **TPTZPSe** are sensitive to the dielectrics of the solvent medium; as the solvent polarity increased from hexane to methanol, the emission peaks were red-shifted (Fig. S15†). All the compounds showed single exponential decay with nanosecond lifetime in the solution state, confirming the emission originating from the singlet excited state (Table S3†). In the case of **TPTZPO**, the lifetime of the species is insensitive to the polarity of the solvent matrix as observed in the solvent dielectric dependent PL spectrum (Fig. S16†). However, the PL lifetimes of **TPTZPS** and **TPTZPSe** increased with increasing solvent polarity, and a longer lifetime was observed for DCM solutions (Table S3†). Based on these results, we concluded that these compounds are weakly emissive in solutions and the PL features of these compounds have their origin from single molecular species. Further, the excited state of **TPTZPO** is nonpolar, while **TPTZPS** and **TPTZPSe** emit from a polar excited state. TD-DFT results are also supportive of these claims (*vide infra*).

Like in the solution state, the pristine solids of **TPTZPO**, **TPTZPS**, and **TPTZPSe** showed a broad PL with λ_{max} at 424, 476, and 463 nm, respectively. In contrast, the solid-state PL spectra of **TPTZPO** and **TPTZPS** red-shifted compared to their respective

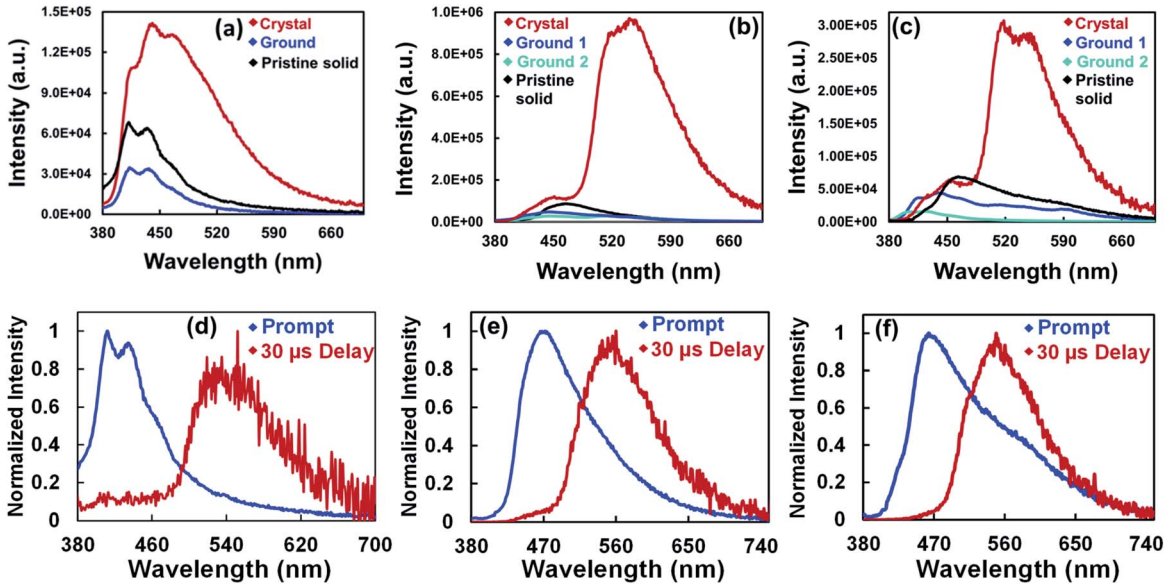

Fig. 3 Photoluminescence spectra (λ_{ex} = 360 nm) of crystals, ground samples, and pristine samples of (a) TPTZPO, (b) TPTZPS and (c) TPTZPSe (Ground 1 indicates grinding with a mortar and pestle for 5 minutes, and Ground 2 indicates heavy grinding for 15 minutes). Prompt and phosphorescence spectra of pristine solids of (d) TPTZPO, (e) TPTZPS, and (f) TPTZPSe, λ_{ex} = 360 nm with 30 μs delay time.

solution spectra except for **TPTZPSe**, in which the PL maximum is blue-shifted compared to its solution spectra. Compounds **TPTZPS** and **TPTZPSe** show larger Stokes shift than **TPTZPO**, which can be attributed to the greater P = X (X = S and Se) resonance length in the former than that in the latter (P═O) (Fig. 2c). The excitation spectra of these compounds show a band at ~360 nm, which is ~60 nm red-shifted compared to the solution absorption maxima (Fig. S17†), indicating that the emissive species in the solid-state is different from that in solution.

Crystalline solids of these compounds showed two PL bands, one at the blue end of the spectra as observed in the pristine solid and a new strong band at the green end of the spectrum (Fig. 3a–c and S18†). The lower energy bands of **TPTZPS** and **TPTZPSe** are red-shifted compared to those of **TPTZPO**. The ground solids of these compounds did not show the lower energy band at the green end of the spectrum and showed the PL band corresponding to their pristine solids. Higher PL quantum yield (PLQY) was measured for the crystals of **TPTZPS** (19.14%) and **TPTZPSe** (7.51%) compared to their pristine solids (**TPTZPS**, 6.53% and **TPTZPSe**, 0.60%). Surprisingly, **TPTZPO** crystals (PLQY = 0.01%) and pristine solids (PLQY = 0.57%) are less emissive than **TPTZPS** and **TPTZPSe**. Further, **TPTZPS** and **TPTZPSe** exhibited considerably higher PLQY than previously reported RTP co-crystals.[101,102]

Powder X-ray diffraction (PXRD) traces of these compounds before and after grinding were recorded (Fig. S19†). The crystals of these compounds showed strong peaks, while the ground samples showed few diffused diffraction peaks. Based on the PL spectra, PLQY, and PXRD studies, it is appropriate to say that the phase change from crystalline to amorphous is responsible for the emission color changes in these compounds.

The fluorescence and phosphorescence spectra of all the compounds were recorded at both ambient and low temperature. DCM solutions of these compounds did not show delayed spectra under ambient conditions. However, the pristine solids, crystals, ground samples, and thin films of these compounds showed distinct prompt and delayed spectra under ambient conditions. The delayed spectra of these compounds are 100 nm red-shifted compared to their fluorescence spectra (Fig. 3d–f, 5 and S26†). The delayed peak position of these compounds smoothly overlapped with the intense lower energy band of the respective crystals.

Nanosecond lifetime was obtained for the higher energy fluorescence bands (Fig. S20, Table S4†). In contrast, incomplete decay was observed for the lower energy band, suggesting long-lived emissive species (Fig. 2d). Furthermore, under an O_2 atmosphere, the delayed emission band nearly vanished, and the prompt spectra remains unchanged. The delayed PL band was restored when the oxygenated samples were purged with N_2 for 5 minutes (Fig. 4b, c and S21†). Furthermore, the delayed emission band decays much faster under an oxygen atmosphere than under a N_2 atmosphere (Fig. S22, Table S5†). However, the fluorescence lifetime showed little change under N_2 and O_2 conditions (Fig. S24, Table S6†). These results indicated that the triplet excited state is involved in the radiative process of these compounds.

To get further insight into the nature of the excited electronic states, the PL spectra of these compounds were collected in the temperature range from 77 K to 298 K. The PL intensity of these compounds progressively increased with lowering the sample temperature from 298 to 77 K. The PL lifetime of these compounds increased significantly at 77 K compared to that at 298 K, which directly corroborates the strong luminescence observed for these compounds at low temperature (Fig. 5b–

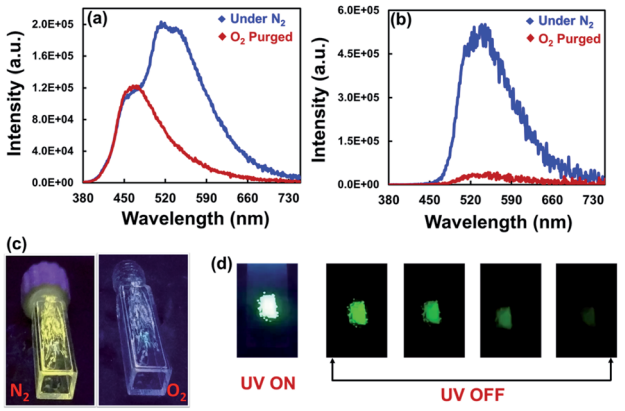

Fig. 4 (a) Prompt spectra, λ_{ex} = 360 nm and (b) phosphorescence spectra of the thin film of **TPTZPS**, with 30 μs delay obtained using a microsecond flash lamp, λ_{ex} = 360 nm. (c) Digital photographs of the thin film of **TPTZPS** under N_2 and O_2 atmospheres under a 365 nm UV lamp. (d) Digital photographs of crystals of **TPTZPS** under 365 nm UV light under on and off conditions (photographs are extracted from a video recorded in a REDMI NOTE 8 PRO mobile).

d and Table S7†). The crystalline solids showed a longer lifetime than the corresponding pristine solids (Fig. 5 and S25†). However, the triplet excited state lifetimes for these phosphoramides are found to be less than those of the previously reported RTP co-crystals.[101,102]

The crystalline solid of **TPTZPS** showed yellowish-green fluorescence under 365 nm UV light illumination followed by green phosphorescence emission after removing the light source, as shown in Fig. 4d. The following conclusions were drawn based on the steady-state and time-resolved emission studies. In the solution state, these compounds exhibit only fluorescence. In the solid-state (both pristine and crystalline solids), they exhibit dual fluorescence and phosphorescence at room temperature.

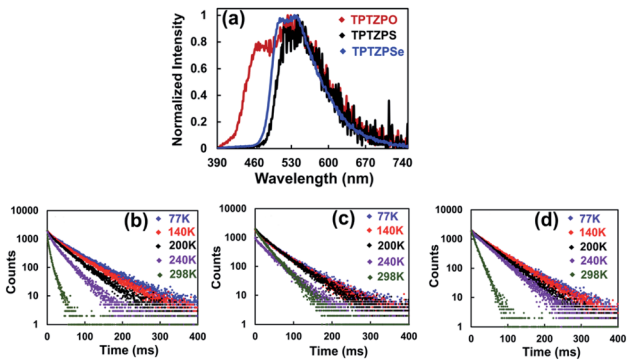

Fig. 5 (a) Phosphorescence spectra of crystals of **TPTZPO**, **TPTZPS** and **TPTZPSe**, λ_{ex} = 360 nm with 30 μs delay obtained using a microsecond flash lamp. Phosphorescence decay profiles of (b) **TPTZPO**, (c) **TPTZPS** and (d) **TPTZPSe** in the crystalline state at different temperatures with 30 μs delay (λ_{ex} = 360 nm and λ_{em} = 550 nm). The lifetimes obtained for crystals of **TPTZPO**, **TPTZPS**, and **TPTZPSe** are 61.03, 53.33, and 58.38 ms, respectively, at 77 K. The lifetime at different temperatures are listed in the ESI, Table S6.†

The phosphorescence lifetime and the PL intensity observed for crystalline solids are significantly larger than those of the corresponding pristine samples (Fig. 5 and S25†). Furthermore, for the crystalline solids, both the lifetime and intensity of the phosphorescence decreased significantly upon ball-milling (Fig. S26 and S27†). These results suggest that the intermolecular interactions in the solid-state effectively inhibit the vibrational deactivation of triplet states; consequently, intense phosphorescence was observed for crystalline solids (Fig. S9–S11†). These characteristics of **TPTZPO**, **TPTZPS** and **TPTZPSe** are in line with the crystallization-induced phosphorescence observed for organic/organometallic compounds reported in the literature.[34,101–103]

It is imperative to note that the positions of the phosphorescence band for the crystals of **TPTZPO**, **TPTZPS**, and **TPTZPSe** are the same, except for a higher energy shoulder band of **TPTZPO** (Fig. 5a). These results indicate that the luminescence of these compounds is centered on the phenothiazine moiety. The shoulder band decays much faster than the phosphorescence band in the lower energy region. The most rapid decay of the blue shoulder phosphorescence of **TPTZPO** may be attributed to the TTA (triplet–triplet annihilation) emission.[104–106] These observations are in line with the PL characteristics of other phenothiazine derivatives reported by Dias *et al.*[86,87]

2.3 Circularly polarized luminescence (CPL) studies

Circularly polarized luminescent (CPL) materials have attracted much attention in recent years because of their potential applications in niche technologies such as 3D displays, information storage, spintronics devices, biological probes, *etc.*[107–112] Compounds **TPTZPS** and **TPTZPSe** crystallized in enantiomerically pure form, and their CPL characteristics were studied. The CPL spectra of these compounds were collected in the fluorescence mode. Upon excitation with 360 nm light, solids of **TPTZPO** show no CPL signals as it is crystallized in the centrosymmetric crystal lattice. However, ground samples of **TPTZPSe** exhibit strong CPL bands at ~460 nm under identical conditions (Fig. S28†). The luminescence dissymmetry factor (g_{lum}) values obtained for **TPTZPSe** (2.7×10^{-3}) are comparable to those obtained for CPL active organic luminophores reported elsewhere.

The crystalline solids of **TPTZPSe** (g_{lum} value = 3.4×10^{-3}) showed the CPL band; surprisingly, no CPL signal was observed for the crystals and ground samples of **TPTZPS** (Fig. 6).

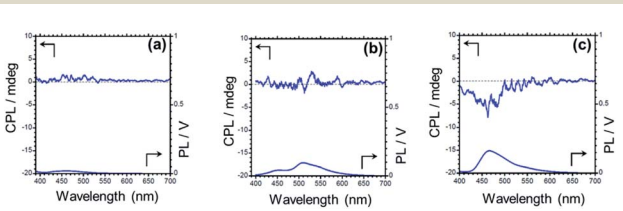

Fig. 6 Circularly polarized luminescence (CPL) spectra and the corresponding photoluminescence spectra of crystals of **TPTZPO** (a), **TPTZPS** (b), and **TPTZPSe** (c), λ_{ex} = 360 nm (CPL spectra – top, PL spectra – bottom) ($g_{CPL} = 3.4 \times 10^{-3}$ for **TPTZPSe**).

Theoretically, both TPTZPS and TPTZPSe should exhibit CPL properties. However, as the g_{lum} value of TPTZPS is small and below the detection limit, a CPL spectrum could not be observed for this compound. In crystalline form, both **TPTZPS** and **TPTZPSe** show intense phosphorescence, while the ground samples of these compounds show strong fluorescence. As the CPL spectra were collected in the fluorescence mode, no CPL signal was observed for strongly phosphorescent crystalline solids of **TPTZPS**. Intense CPL activity was observed for the ground sample of **TPTZPSe**, which was strongly fluorescent. However, phosphorescence emission being inherently weak could not be detected in the CPL. No CPL signal was observed for the solutions of these compounds due to fast racemization.

2.4 Theoretical calculations

Computational studies were carried out to gain further insight into the electronic structure and the observed optical properties of these compounds. Both ground (S_0) and excited state (S_1 and T_1) geometries of **TPTZPO**, **TPTZPS**, and **TPTZPSe** were optimized using DFT (B3LYP, 6-31G (d,p)) and TDDFT (CAM-B3LYP and 6-31G(d,p)), respectively. Frontier molecular orbital (HOMO and LUMO) pictures suggested that n–π* and π–π* are the major transitions in these compounds (n orbital of phenothiazine sulfur and heteroatom (O/S/Se) attached to the P center to the π* orbital of phenothiazine) (Fig. 7a). Geometries and bonding parameters of these molecules in the S_0 and S_1 states are very similar to those of the structure obtained by single-crystal X-ray diffraction studies. The T_1 state geometries of **TPTZPO** and **TPTZPSe** molecules are very different from the S_0 and S_1 state geometries (Table S8–S10, Fig. S29†).

In S_0 and S_1 all the phenothiazine units are symmetrically puckered, however, in the T_1 state, one of the three phenothiazines is unsymmetrically puckered; in contrast, the geometry of the other two rings remains unchanged. To accommodate these conformational changes, the P–N bond length is elongated in the T_1 state (Tables S8–S10†) compared to that in S_0 and S_1. However, in the case of **TPTZPS**, the geometries of all three phenothiazine moieties remain unchanged when it goes from the S_1 to T_1 state.

The computed $\Delta E_{S_1T_1}$ values match well with the experimental $\Delta E_{S_1T_1}$ values calculated from the maxima of fluorescence and phosphorescence spectra (Table S11†). Furthermore, high $\Delta E_{S_1T_1}$ values (0.66–0.76 eV) rule out the $S_1 \leftarrow T_1$ RISC and TADF (Fig. 7b, Table S12†). To get insight into the possible ISC pathways, $S_0 \rightarrow T_n$ vertical transitions were calculated. The results showed that higher triplet states are placed close to the S_1 state. Moreover, the commonality of the orbitals involved in the $S_0 \rightarrow S_1$ and $S_0 \rightarrow T_n$ **TPTZPO** ($S_0 \rightarrow T_1$, $S_0 \rightarrow T_{11}$), **TPTZPS** ($S_0 \rightarrow T_1$, $S_0 \rightarrow T_{11}$), and **TPTZPSe** ($S_0 \rightarrow T_7$) transitions suggests that the ISC transition occurs *via* higher triplet states (Tables S13–S15†). Frontier molecular orbital pictures indicated that both S_1 and T_1 states are of n–π* nature (Fig. S30–31†).

To investigate more about excited state dynamics, we calculated the spin density of these molecules in the ground, singlet, and triplet excited states. The spin density pictures of S_0 and S_1 look similar for all three compounds, but the scenario is

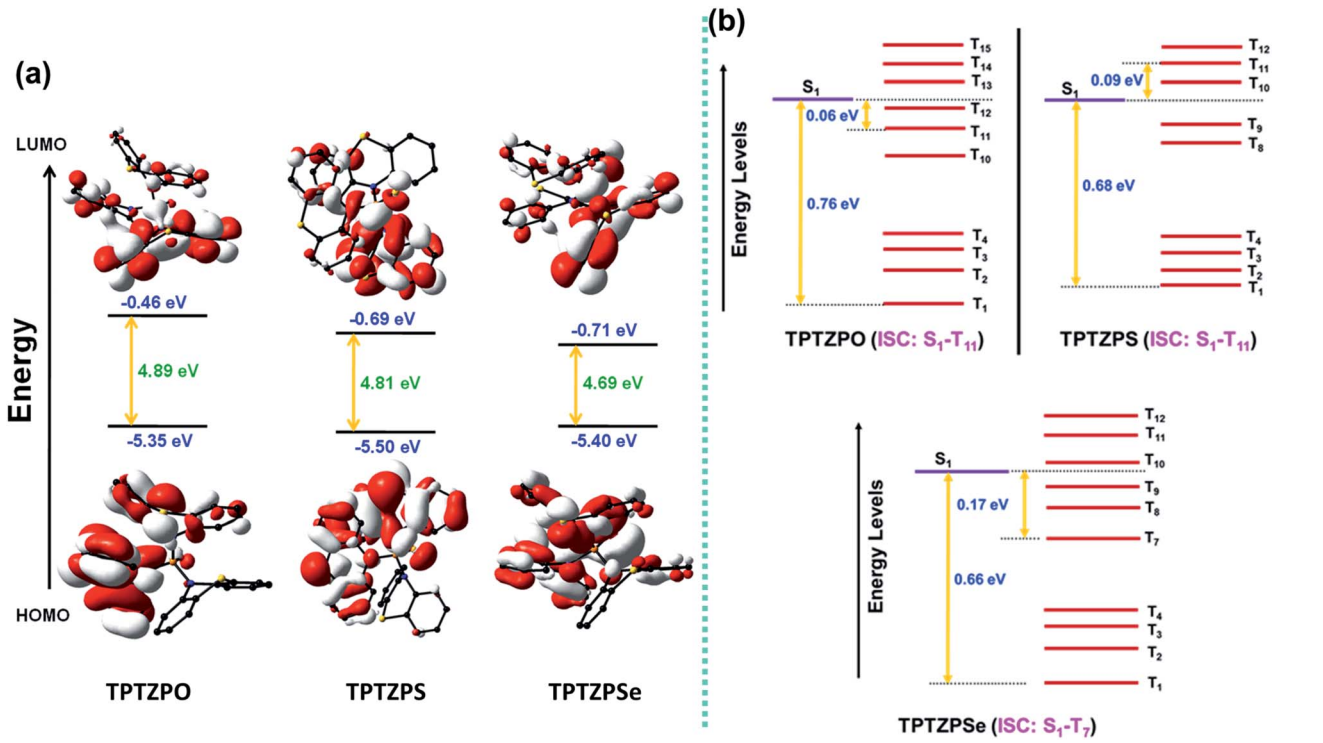

Fig. 7 (a) Frontier molecular orbital energy level diagrams of TPTZPO, TPTZPS, and TPTZPSe (DFT, B3LYP functional with 6-31G (d,p) basis set). (b) Energy level diagram showing the singlet–triplet gap and possible ISC channel of TPTZPO, TPTZPS and TPTZPSe (energy levels in the diagram are not up to scale).

different in the triplet state (T_1) (Fig. S32–S34†). In the triplet state, for **TPTZPO**, the spin density is localized on one of the three phenothiazine moieties (the ring distorted in the triplet state). However, the spin density is delocalized over both phenothiazine and P = X (X = S and Se) in **TPTZPS** and **TPTZPSe**. Thus, **TPTZPS** and **TPTZPSe** show similar phosphorescence features involving n–π* triplet states. However, in **TPTZPO**, the localization of spin density on a single phenothiazine unit and the types of orbitals involved in S_0–T_1 transitions indicate that the phosphorescence is from the triplet having hybridized LE and n–π* states. Thus, **TPTZPO** shows a structured phosphorescence band at a lower wavelength than **TPTZPS** and **TPTZPSe**.

3. Conclusions

In summary, we have designed and synthesized three phosphoramides, **TPTZPO**, **TPTZPS**, and **TPTZPSe**. These compounds show fluorescence in solution and dual fluorescence and RTP in the solid-state (crystalline and amorphous solids). Detailed experimental and computational studies demonstrate that the phosphorescence of these compounds originates from the triplet n–π* state dominated by the phenothiazine moiety. All the compounds exhibit crystallization-induced room-temperature phosphorescence, a phenomenon quite rarely observed for this class of compounds. Moreover, both **TPTZPS** and **TPTZPSe** crystallized in the chiral space group; however, only **TPTZPSe** showed CPL signals in the solid-state.

Data availability

Publicly available datasets were analyzed in this study. This data can be found here: (**https://www.ccdc.cam.ac.uk/structures/**) CCDC 1977279, 1916761 and 1916789.†

Author contributions

SJ did compound synthesis, DFT calculations and PL characterization. SB did preliminary PL studies. Both JE and SJ contributed to data analysis. YI and MK did CPL studies. All the authors commented on the manuscript. PT organized the entire project.

Conflicts of interest

There are no conflicts to declare.

Acknowledgements

The authors are thankful to the IISc, DST and SERB for financial support. SJ thanks the Indian Institute of Science Bangalore, JE acknowledges the support from Prime Minister's Research Fellowship (PMRF) and SKB thanks Kothari postdoctoral fellowship of India, The authors thank Prof. Debasis Das for providing the HPLC facility and Kalpana Rajendran for doing the measurements.

References

1 C. W. Tanga and S. A. VanSlyke, *Appl. Phys. Lett.*, 1987, **51**, 913.
2 N. J. Turro, *Modern Molecular Photochemistry*, University Science Books, Sausalito, CA, 1991,Benjamin/Cummings, Menlo Park, NJ, 1978.
3 C. Adachi, M. A. Baldo, M. E. Thompson and S. R. Forrest, *J. Appl. Phys.*, 2001, **90**, 5048–5051.
4 B. Song, W. Shao, J. Jung, S.-J. Yoon and J. Kim, *ACS Appl. Mater. Interfaces*, 2020, **12**, 6137–6143.
5 Y. Kawamura, K. Goushi, J. Brooks, J. J. Brown, H. Sasabe and C. Adachi, *Appl. Phys. Lett.*, 2005, **86**, 071104.
6 E. Holder, B. M. W. Langeveld and U. S. Schubert, *Adv. Mater.*, 2005, **17**, 1109–1121.
7 S. J. Su, T. Chiba, T. Takeda and J. Kido, *Adv. Mater.*, 2008, **20**, 2125–2130.
8 H. F. Higginbotham, M. Okazaki, P. de Silva, S. Minakata, Y. Takeda and P. Data, *ACS Appl. Mater. Interfaces*, 2021, **13**, 2899–2907.
9 S. Hu, J. Zeng, X. Zhu, J. Guo, S. Chen, Z. Zhao and B. Z. Tang, *ACS Appl. Mater. Interfaces*, 2019, **11**, 27134–27144.
10 J. M. Vanderkooi, G. Maniara, T. J. Green and D. F. Wilson, *J. Biol. Chem.*, 1987, **262**, 5476–5482.
11 R. Gao, D. G. Ho, B. Hernandez, M. Selke, D. Murphy, P. I. Djurovich and M. E. Thompson, *J. Am. Chem. Soc.*, 2002, **124**, 14828–14829.
12 M. C. DeRosa, D. J. Hodgson, G. D. Enright, B. Dawson, C. E. B. Evans and R. J. Crutchley, *J. Am. Chem. Soc.*, 2004, **126**, 7619–7626.
13 S. M. Borisov, G. Zenkl and I. Klimant, *ACS Appl. Mater. Interfaces*, 2010, **2**, 366–374.
14 A. Pfister, G. Zhang, J. Zareno, A. F. Horwitz and C. L. Fraser, *ACS Nano*, 2008, **2**, 1252–1258.
15 N. Gan, H. Shi, Z. An and W. Huang, *Adv. Funct. Mater.*, 2018, **28**, 1802657.
16 G. Zhang, G. M. Palmer, M. W. Dewhirst and C. L. Fraser, *Nat. Mater.*, 2009, **8**, 747–751.
17 Q. Zhao, C. Huang and F. Li, *Chem. Soc. Rev.*, 2011, **40**, 2508–2524.
18 X. Chen, C. Xu, T. Wang, C. Zhou, J. Du, Z. Wang, H. Xu, T. Xie, G. Bi, J. Jiang, X. Zhang, J. N. Demas, C. O. Trindle, Y. Luo and G. Zhang, *Angew. Chem., Int. Ed.*, 2016, **55**, 9872–9876.
19 N. Gan, H. Shi, Z. An and W. Huang, *Adv. Funct. Mater.*, 2018, **28**, 1802657.
20 R. Kabe and C. Adachi, *Nature*, 2017, **550**, 384–387.
21 R. Kumar, T. Y. Ohulchanskyy, I. Roy, S. K. Gupta, C. Borek, M. E. Thompson and P. N. Prasad, *ACS Appl. Mater. Interfaces*, 2009, **1**, 1474–1481.
22 A. Tsuboyama, H. Iwawak, M. Furugori, T. Mukaide, J. Kamatani, S. Igawa, T. Moriyama, S. Miura, T. Takiguchi, S. Okada, M. Hoshino and K. Ueno, *J. Am. Chem. Soc.*, 2003, **125**, 12971–12979.
23 Y. J. Su, H. L. Huang, C. L. Li, C. H. Chien, Y. T. Tao, P. T. Chou, S. Datta and R. S. Liu, *Adv. Mater.*, 2003, **15**, 884–888.

24 Y. You and S. Y. Park, *Dalton Trans.*, 2009, 1267–1282.
25 J. Brooks, Y. Babayan, S. Lamansky, P. I. Djurovich, I. Tsyba, R. Bau and M. E. Thompson, *Inorg. Chem.*, 2002, **41**, 3055–3066.
26 Y. Y. Lin, S. C. Chan, M. C. W. Chan, Y. J. Hou, N. Zhu, C. M. Che, Y. Liu and Y. Wang, *Chem.–Eur. J.*, 2003, **9**, 1263–1272.
27 X. L. Yang, C. L. Yao and G. J. Zhou, *Platinum Met. Rev.*, 2013, **57**, 2–16.
28 W. Lu, N. Zhu and C. M. Che, *J. Am. Chem. Soc.*, 2003, **125**, 16081–16088.
29 M. Osawa, M. Hoshino, M. Akita and T. Wada, *Inorg. Chem.*, 2005, **44**, 1157–1159.
30 H. Rudmann, S. Shimada and M. F. Rubner, *J. Am. Chem. Soc.*, 2002, **124**, 4918–4921.
31 H. V. R. Dias, H. V. K. Diyabalanage, M. A. R. Omary, M. A. Franzman and M. A. Omary, *J. Am. Chem. Soc.*, 2003, **125**, 12072–12073.
32 C.-L. Ho, W.-Y. Wong, Z.-Q. Gao, C.-H. Chen, K.-W. Cheah, B. Yao, Z. Xie, Q. Wang, D. Ma, L. Wang, X.-M. Yu, H.-S. Kwok and Z. Lin, *Adv. Funct. Mater.*, 2008, **18**, 319–331.
33 A. B. Alemayehu, N. U. Day, T. Mani, A. B. Rudine, K. E. Thomas, O. A. Gederaas, S. A. Vinogradov, C. C. Wamser and A. Ghosh, *ACS Appl. Mater. Interfaces*, 2016, **8**, 18935–18942.
34 J. Yang, X. Gao, Z. Xie, Y. Gong, M. Fang, Q. Peng, Z. Chi and Z. Li, *Angew. Chem., Int. Ed.*, 2017, **56**, 15299–15303.
35 Y. Xiong, Z. Zhao, W. Zhao, H. Ma, Q. Peng, Z. He, X. Zhang, Y. Chen, X. He, J. W. Y. Lam and B. Z. Tang, *Angew. Chem., Int. Ed.*, 2018, **57**, 7997–8001.
36 O. Bolton, K. Lee, H. J. Kim, K. Y. Lin and J. Kim, *Nat. Chem.*, 2011, **3**, 205–210.
37 M. Baroncini, G. Bergamini and P. Ceroni, *Chem. Commun.*, 2017, **53**, 2081–2093.
38 D. Lee, O. Bolton, B. C. Kim, J. H. Youk, S. Takayama and J. Kim, *J. Am. Chem. Soc.*, 2013, **135**, 6325–6632.
39 Y. Xie, Y. Ge, Q. Peng, C. Li, Q. Lia and Z. Li, *Adv. Mater.*, 2017, **29**, 1606829.
40 S. Hirata, K. Totani, J. Zhang, T. Yamashita, H. Kaji, S. R. Marder, T. Watanabe and C. Adachi, *Adv. Funct. Mater.*, 2013, **23**, 3386–3397.
41 W. Zhao, Z. He and B. Z. Tang, *Nat. Rev. Mater.*, 2020, **5**, 869–885.
42 Kenry, C. Chen and B. Liu, *Nat. Commun.*, 2019, **10**, 2111.
43 H. Wu, L. Gu, G. V. Baryshnikov, H. Wang, B. F. Minaev, H. Ågren and Y. Zhao, *ACS Appl. Mater. Interfaces*, 2020, **12**, 20765–20774.
44 T. Virgili, A. Forni, E. Cariati, D. Pasini and C. Botta, *J. Phys. Chem. C*, 2013, **117**, 27161–27166.
45 R. Gao, M. S. Kodaimati and D. Yan, *Chem. Soc. Rev.*, 2021, **50**, 5564–5589.
46 X. Yang and D. Yan, *Chem. Sci.*, 2016, **7**, 4519–4526.
47 D. Yan and D. G. Evans, *Mater. Horiz.*, 2014, **1**, 46–57.
48 S. Mukherjee and P. Thilagar, *Chem. Commun.*, 2015, **51**, 10988–11003.
49 G. Zhang, J. Chen, S. J. Payne, S. E. Kooi, J. N. Demas and C. L. Fraser, *J. Am. Chem. Soc.*, 2007, **129**, 8942–8943.
50 S. Kawai, S. Saito, S. Osumi, S. Yamaguchi, A. S. Foster, P. Spijker and E. Meyer, *Nat. Commun.*, 2015, **6**, 1–6.
51 Z. Chai, C. Wang, J. Wang, F. Liu, Y. Xie, Y. Z. Zhang, J. R. Li, Q. Li and Z. Li, *Chem. Sci.*, 2017, **8**, 8336–8344.
52 Y. Shoji, Y. Ikabata, Q. Wang, D. Nemoto, A. Sakamoto, N. Tanaka, J. Seino, H. Nakai and T. Fukushima, *J. Am. Chem. Soc.*, 2017, **139**, 2728–2733.
53 Y. Ren and F. Jakle, *Dalton Trans.*, 2016, **45**, 13996–14007.
54 M. Shimizu, R. Shigitani, M. Nakatani, K. Kuwabara, Y. Miyake, K. Tajima, H. Sakai and T. Hasobe, *J. Phys. Chem. C*, 2016, **120**, 11631–11639.
55 V. Chandrasekhar, M. D. Pandey, B. Das, B. Mahanti, K. Gopal and R. Azhakar, *Tetrahedron*, 2011, **67**, 6917–6926.
56 V. Chandrasekhar, R. Azhakar, J. F. Bickley and A. Steiner, *Cryst. Growth Des.*, 2006, **6**, 910–914.
57 T. Baumgartner and R. Réau, *Chem. Rev.*, 2006, **106**, 4681–4727.
58 M. Stolar and T. Baumgartner, *Chem.–Asian J.*, 2014, **9**, 1212–1225.
59 F. M. Xie, Q. Ou, Q. Zhang, J. K. Zhang, G. L. Dai, X. Zhao and H. X. Wei, *Beilstein J. Org. Chem.*, 2018, **14**, 869–874.
60 J. Yang, X. Zhen, B. Wang, X. Gao, Z. Ren, J. Wang, Y. Xie, J. Li, Q. Peng, K. Pu and Z. Li, *Nat. Commun.*, 2018, **9**, 1–10.
61 Y. Ren, M. Sezen, F. Guo, F. Jakle and Y. L. Loo, *Chem. Sci.*, 2016, **7**, 4211–4219.
62 Y. Tao, J. Xiao, C. Zheng, Z. Zhang, M. Yan, R. Chen, X. Zhou, H. Li, Z. An, Z. Wang, H. Xu and W. Huang, *Angew. Chem., Int. Ed.*, 2013, **52**, 10491–10495.
63 T. Ye, L. Xu, Z. Zhang, R. Chen, H. Li, H. Xu, C. Zheng and W. Huang, *J. Am. Chem. Soc.*, 2016, **138**, 9655–9662.
64 F. Gao, R. Du, C. Han, J. Zhang, Y. Wei, G. Lu and H. Xu, *Chem. Sci.*, 2019, **10**, 5556–5567.
65 Z. An, C. Zheng, Y. Tao, R. Chen, H. Shi, T. Chen, Z. Wang, H. Li, R. Deng, X. Liu and W. Huang, *Nat. Mater.*, 2015, **14**, 685–690.
66 W. Z. Yuan, X. Y. Shen, H. Zhao, J. W. Y. Lam, L. Tang, P. Lu, C. Wang, Y. Liu, Z. Wang, Q. Zheng, J. Z. Sun, Y. Ma and B. Z. Tang, *J. Phys. Chem. C*, 2010, **114**, 136090–136099.
67 P. Pander, A. Swist, J. Soloducho and F. B. Dias, *Dyes Pigm.*, 2017, **142**, 315–322.
68 P. Pander, A. Swist, R. Turczyn, S. Pouget, D. Djurado, A. Lazauskas, R. Pashazadeh, J. V. Grazulevicius, R. Motyka, A. Klimash, P. J. Skabara, P. Data, J. Soloducho and F. B. Dias, *J. Phys. Chem. C*, 2018, **122**, 24958–24966.
69 S. O. Jeon, K. S. Yook, C. W. Joo and J. Y. Lee, *Adv. Funct. Mater.*, 2009, **19**, 3644–3649.
70 C. Fan, C. Duan, Y. Wei, D. Ding, H. Xu and W. Huang, *Chem. Mater.*, 2015, **27**, 5131–5140.
71 C. Fan, C. Duan, C. Han, B. Han and H. Xu, *ACS Appl. Mater. Interfaces*, 2016, **8**, 27383–27393.
72 C. Zhou, S. Zhang, Y. Gao, H. Liu, T. Shan, X. Liang, B. Yang and Y. Ma, *Adv. Funct. Mater.*, 2018, **28**, 1802407.
73 X. Bi, Y. Shi, T. Peng, S. Yue, F. Wang, L. Zheng and Q.-E. Cao, *Adv. Funct. Mater.*, 2021, **31**, 2101312.
74 W. Zhao, T. S. Cheung, N. Jiang, W. Huang, J. W. Y. Lam, X. Zhang, Z. He and B. Z. Tang, *Nat. Commun.*, 2019, **10**, 1595.

75 L. Ma, S. Sun, B. Ding, X. Ma and H. Tian, *Adv. Funct. Mater.*, 2021, **31**, 2010659.
76 R. Chen, Y. Guan, H. Wang, Y. Zhu, X. Tan, P. Wang, X. Wang, X. Fan and H.-L. Xie, *ACS Appl. Mater. Interfaces*, 2021, **13**, 41131–41139.
77 S. Tian, H. Ma, X. Wang, A. Lv, H. Shi, Y. Geng, J. Li, F. Liang, Z. M. Su, Z. An and W. Huang, *Angew. Chem., Int. Ed.*, 2019, **58**, 6645–6649.
78 P. C. A. Swamy, S. Mukherjee and P. Thilagar, *Chem. Commun.*, 2013, **49**, 993–995.
79 S. K. Sarkar and P. Thilagar, *Chem. Commun.*, 2013, **49**, 8558–8560.
80 P. C. A. Swamy, S. Mukherjee and P. Thilagar, *Inorg. Chem.*, 2014, **53**, 4813–4823.
81 K. N. Kalluvettukuzhy, S. Pagidi, D. Kumbhar and P. Thilagar, *Chem. Commun.*, 2017, **53**, 3641–3644.
82 S. Mukherjee and P. Thilagar, *Phys. Chem. Chem. Phys.*, 2014, **16**, 20866–20877.
83 S. Mukherjee and P. Thilagar, *Chem.–Eur. J.*, 2014, **20**, 8012–8023.
84 Z. Xei, C. Chen, S. Xu, J. Li, Y. Zhang, S. Liu, J. Xu and Z. Chi, *Angew. Chem., Int. Ed.*, 2015, **54**, 7181–7184.
85 J. Guo, X. L. Li, H. Nie, W. Luo, R. Hu, A. Qin, Z. Zhao, S. J. Su and B. Z. Tang, *Chem. Mater.*, 2017, **29**, 3623–3631.
86 F. B. Dias, J. Santos, D. R. Graves, P. Data, R. S. Nobuyasu, M. A. Fox, A. S. Batsanov, T. Palmeira, M. N. Berberan-Santos, M. R. Bryce and A. P. Monkman, *Adv. Sci.*, 2016, **3**, 1600080.
87 J. S. Ward, R. S. Nobuyasu, A. S. Batsanov, P. Data, A. P. Monkman, F. B. Dias and M. R. Bryce, *Chem. Commun.*, 2016, **52**, 2612–2615.
88 M. Okazaki, Y. Takeda, P. Data, P. Pander, H. Higginbotham, A. P. Monkman and S. Minakata, *Chem. Sci.*, 2017, **8**, 2677–2686.
89 S. Gan, W. Luo, B. He, L. Chen, H. Nie, R. Hu, A. Qin, Z. Zhao and B. Z. Tang, *J. Mater. Chem. C*, 2016, **4**, 3705–3708.
90 C. Chen, R. Huang, A. S. Batsanov, P. Pander, Y. T. Hsu, Z. Chi, F. B. Dias and M. R. Bryce, *Angew. Chem., Int. Ed.*, 2018, **130**, 16645–16649.
91 H. Tanaka, K. Shizu, H. Nakanotani and C. Adachi, *J. Phys. Chem. C*, 2014, **118**, 15985–15994.
92 P. Pander, A. Swist, R. Motyka, J. Soloducho, F. B. Dias and P. Data, *J. Mater. Chem. C*, 2018, **6**, 5434–5443.
93 J. Yang, H. Gao, Y. Wang, Y. Yu, Y. Gong, M. Fang, D. Ding, W. Hu, B. Z. Tang and Z. Li, *Mater. Chem. Front.*, 2019, **3**, 1391–1397.
94 Y. Wang, J. Yang, M. Fang, Y. Gong, J. Ren, L. Tu, B. Z. Tang and Z. Li, *Adv. Funct. Mater.*, 2021, **31**, 2101719.
95 Z. Zhao, G. Yu, Q. Chang, X. Liu, Y. Liu, L. Wang, Z. Liu, Z. Bian, W. Liu and C. Huang, *J. Mater. Chem. C*, 2017, **5**, 7344–7351.
96 A. D. Burrows, G. K. Köhn, M. F. Mahon and M. Varrone, *C. R. Chim.*, 2006, **9**, 111–119.
97 H. S. Gutowsky and C. H. Holm, *J. Chem. Phys.*, 1956, **25**, 1228–1234.
98 H. Jiang, L. Jia, Y. Li, S. Liu, R. Chen, L. Jin, J. Jin, C. Zheng, F. Fan and W. Huang, *Chem. Commun.*, 2017, **53**, 3641–3644.
99 J. P. Majoral and A. M. Caminade, *Chem. Rev.*, 1999, **99**, 845–880.
100 T. Nishimoto, T. Yasuda, S. Y. Lee, R. Kondo and C. Adachi, *Mater.Horiz.*, 2014, **1**, 264–269.
101 B. Zhou, Q. Zhao, L. Tanga and D. Yan, *Chem. Commun.*, 2020, **56**, 7698–7701.
102 B. Zhou and D. Yan, *Adv. Funct. Mater.*, 2019, **29**, 1807599.
103 A. Nitti, C. Botta, A. Forni, E. Cariati, E. Lucenti and D. Pasini, *CrystEngComm*, 2020, **22**, 7782–7785.
104 H. Sternlicht, G. C. Nieman and G. W. Robinson, *J. Chem. Phys.*, 1963, **38**, 1326.
105 M. Shao, L. Yan, M. Li, I. Ilia and B. Hu, *J. Mater. Chem. C*, 2013, **1**, 1330–1336.
106 Y. Zhang and S. R. Forrest, *Chem. Phys. Lett.*, 2013, **590**, 106–110.
107 J. J. Maki, T. Verbiest, M. Kauranen, S. V. Elshocht and A. Persoons, *J. Chem. Phys.*, 1996, **105**, 767.
108 R. Tempelaar, A. Stradomska, J. Knoester and F. C. Spano, *J. Phys. Chem. B*, 2011, **115**, 10592.
109 W. B. Sparks, J. Hough, T. A. Germer, F. Chen, S. DasSarma, P. DasSarma, F. T. Robb, N. Manset, L. Kolokolova, N. Reid, F. D. Macchetto and W. Martin, *Proc. Natl. Acad. Sci. U. S. A.*, 2009, **106**, 7816.
110 S. W. Huo, P. F. Duan, T. F. Jiao, Q. M. Peng and M. H. Liu, *Angew. Chem., Int. Ed.*, 2017, **56**, 12174–12178.
111 X. Yang, X. Lin, Y. Zhao, Y. S. Zhao and D. Yan, *Angew. Chem., Int. Ed.*, 2017, **56**, 7853–7857.
112 A. Nitti and D. Pasini, *Adv. Mater.*, 2020, **32**, 1908021.